

Histological and Immunohistochemical Assessment of the Impact of Geraniol on Tartrazine Induced Histopathological Alterations in The Exocrine Pancreas of Adult Male Albino Rat

Maram Mohamed Elkelany and Dina Fouad El Shaer

Department of Histology and Cell Biology, Faculty of Medicine, Tanta University, Egypt

ABSTRACT

Introduction: Tartrazine (TZ) is an azobenzene synthetic food coloring dye that is most widely used in the drug, cosmetic, and food industries. In spite of its numerous health hazards and toxic effects, the impact of tartrazine exposure on the exocrine pancreas is still to be illustrated. Geraniol (GE) is a plant-derived natural bioactive compound that is a common ingredient in essential oils of several plants. It has antioxidant, antimicrobial, antibacterial, anti-inflammatory properties, and numerous health benefits.

Objectives: This study aimed to demonstrate the impact of geraniol against tartrazine-induced histopathological alterations in the exocrine pancreatic tissue in adult male albino rats.

Materials and Methods: 45 rats were divided into 4 groups: the control group, GE-group (received 200 mg/kg/day GE orally for 30 days), TZ-group (received 300 mg/kg/day TZ orally for 30 days), and TZ&GE-group (received TZ and GE concomitantly at the same dose and duration as previous groups). The pancreatic tissues were dissected and prepared for histological and immunohistochemical study.

Results: TZ-group revealed acinar cells with pyknotic nuclei, perinuclear haloes, vacuolated cytoplasm, loss of basal cytoplasmic basophilia, and scanty zymogen granules. Further, dilated ducts with retained secretion, dilated congested blood vessels, inflammatory cellular infiltration, and excessive collagen deposition were recognized. Ultrastructurally, irregular dark nuclei with dilated perinuclear space, vacuolated cytoplasm, dilated rER cisternae, zymogen granules' alterations, and wide intercellular spaces were seen in the TZ-group. Tartrazine also caused increased VEGF immunoreactivity. Geraniol coadministration ameliorated these histological changes.

Conclusion: Geraniol has an ameliorating effect against the deleterious effects of tartrazine on the exocrine pancreas of adult male albino rats.

Received: 07 September 2022, **Accepted:** 04 October 2022

Key Words: Exocrine pancreas, geraniol, tartrazine, ultrastructure, VEGF.

Corresponding Author: Dina Fouad El Shaer, MD, Department of Histology and Cell Biology, Faculty of Medicine, Tanta University, Egypt, **Tel.:** +20 12 2434 7776, **E-mail:** dinaelshaer@yahoo.com

ISSN: 1110-0559, Vol. 46, No. 4

INTRODUCTION

The food additives, including the synthetic food azo-dyes, are widely consumed to improve the color and taste of several food products. The food azo-dyes consist of azo functional groups and aromatic ring structures, which have adverse effects on the human body^[1]. Tartrazine (TZ) is a yellow to orange synthetic acid azo-dye that is widely used as a food coloring substance and in food additives, sugar coating, pastry, candy, beverages as well as in drug industries. Consumption of tartrazine either directly or as an ingredient in the food for a long duration may cause allergy, migraine, eczema, anxiety, and troubles in the digestive system as well as an increase in the blood glucose level. Moreover, tartrazine overconsumption may accumulate in the body causing kidney and liver failure. Further, tartrazine has adverse effects on children as it can cause allergic reactions, hyperactivity, and sleep disorders^[2,3].

Nowadays, tartrazine is extensively used not only in our daily food products but also in non-food stuff. The

allowed consumption of tartrazine for humans is 0-7.5 mg/ kg.bw/day^[4]. Recently, it was reported that tartrazine consumption even at the acceptable daily intake level (ADI) may cause several health hazards, including genotoxicity, embryotoxicity, and even carcinogenicity. When tartrazine is orally taken, it is subjected to the azo reduction in the gut and liver causing the release of aromatic amine sulfanilic acid and aminopyrazolone which leads to the release of excessive reactive oxygen species (ROS) that cross the blood brain barrier (BBB) leading to oxidative stress, which in return causes organ and tissue damages^[5,6].

Pancreas tissues are more susceptible to oxidative stress than other organs due to the fragility of their internal anti-oxidative system. Numerous factors such as drugs, chemicals, viruses, and trauma can induce pancreatic insult either directly or indirectly which in turn may affect its function^[7,8].

Geraniol (GE) (3,7-dimethyl-2, 6-octadien-1-ol) is a clear or pale yellow acyclic monoterpene alcohol oil that is soluble in most organic solvents but insoluble in

water. More than 250 essential oils contain geraniol as a fundamental component, such as monarda fistulosa oil, ninde oil, rose oil, and palmarosa oil^[9]. It is commonly used in spices, detergents, shampoos, soaps, cosmetics, and perfumes. Geraniol has a broad spectrum of pharmacological activities as antimicrobial, anti-inflammatory, antibacterial, antioxidant, antiulcer, hepatoprotective, anticancer, and anthelmintic^[10]. Moreover, geraniol is used in the treatment of various diseases such as cancer, diabetes, and neurological disorders. The Food and Drug Administration (FDA) designated it as GRAS (Generally Recognized as Safe), to be utilized in flavoring and for safe human consumption^[11].

Previous studies illustrated the toxic effect of tartrazine on public health and some studies demonstrated its effect on the endocrine system and metabolic disorders. However, until now, few limited studies have been performed to investigate the effect of tartrazine on the exocrine portion of the pancreas particularly. Hence, we aimed to evaluate the effect of tartrazine exposure on the exocrine portion of the normal functioning pancreas in adult male albino rats. Furthermore, we also aimed to investigate the possible ameliorating effect of geraniol on tartrazine-induced hazards.

MATERIALS AND METHODS

Experimental Animals

Forty-five adult male Wistar albino rats aged 10-13 weeks old and weighing 190-220 g. were used in this experiment. The experimental animals were subjected to suitable laboratory conditions and were fed standard laboratory animal feed with free access to water. Rats were left for a week to acclimatize to their new environment before starting the experiment.

The experiment was carried out in the animal house of the Histology and Cell Biology Department in the Faculty of Medicine, Tanta University. The experimental design and handling procedures were performed according to the guideline of the Ethics Committee of Tanta University (Approval number: 35658/8/22).

Chemical Reagents

Tartrazine was purchased in the form of yellow to yellow-orange powder from Sigma-Aldrich Chemicals (St. Louis, MO, USA) (CAS-number: 1934-21-0, C₁₆H₉N₄Na₃O₉S₂, Purity 85%). Tartrazine solution was prepared at a concentration of 60mg/1ml by dissolving 3000 mg tartrazine in 50 ml of distilled water.

Geraniol was purchased in the form of colorless liquid from Sigma-Aldrich Chemicals (St. Louis, MO, USA) (CAS-number:106-24-1, C₁₀H₁₈O, 98% purity). Geraniol solution was prepared at a concentration of 40mg/0.9 ml by dissolving a vial of geraniol at a concentration (26.370 gm/30ml) in 570 ml of normal saline.

Animal groups

Forty-five rats were randomly distributed into 4 groups, all the administrations were received orally (via gavage) for consecutive 30 days:

1. Control group (group I): included 15 rats were subdivided randomly into 3 subgroups (each 5 rats) as follows:
 - Subgroup Ia: included 5 rats that were left without any treatment through the experimental period.
 - Subgroup Ib: included 5 rats, each of them was orally given 1% carboxymethyl cellulose (CMC) in 0.9ml normal saline, the diluting vehicle for geraniol^[11].
 - Subgroup Ic: included 5 rats, each of them was orally given 1ml/day of distilled water, the diluting vehicle for tartrazine.
2. GE-group (group II): included 10 rats, each of them orally received 0.9ml of geraniol solution at a dose of 200 mg/kg/day^[11].
3. TZ-group (group III): included 10 rats, each of them orally received 1ml of tartrazine solution at a dose of 300 mg/kg/day^[12].
4. TZ & GE-group (group IV): included 10 rats that were daily concomitantly received geraniol as in group II and tartrazine as in group III.

After 30 days of drugs administration, all rats were anesthetized with sodium pentobarbital at a dose of 50 mg/kg through intraperitoneal injection^[13]. A midline incision in the anterior abdominal wall was done to dissect and excise the pancreas. Each pancreas was cut longitudinally into two halves; one of each was processed for light microscopic study and the other for electron microscopic study.

Preparation for light microscopy examination

Specimens were fixed in 10% formalin fixative solution for 24 hours, dehydrated in ascending grades of ethyl alcohol, cleared in xylene, impregnated then blocked-in paraffin wax to be processed for light microscopic study. Serial paraffin sections (5 µm thickness) were cut and mounted on slides then were stained with hematoxylin and eosin (H&E) and Masson's trichrome (MT) stains^[14].

Immunohistochemical staining

5-µm-thick sections were used for anti-vascular endothelial growth factor (VEGF). Sections were deparaffinized, rehydrated and antigen retrieval was done. Then inactivation of endogenous peroxidase was performed by incubation in 3% hydrogen peroxide followed by washing with PBS. After that, incubation of the slides with diluted (1:100) rabbit monoclonal anti-VEGF antibody (obtained from Biocare Medical Company-USA, Cat. No.: CME 356 AK) was done overnight at 4°C. The sections

were then rinsed with PBS and incubated with biotinylated secondary antibodies for 30 min at room temperature, then washed in PBS. After that sections were incubated with the streptavidin-enzyme conjugate solution. Subsequently, 3,3'-diaminobenzidine (DAB) hydrogen peroxide was used to visualize the immunoreactivity, and tissue sections were counter-stained with hematoxylin. Positive control was from the normal tonsil. The positive reaction under the light microscope appeared as cytoplasmic brown particles or patches. Negative control was run automatically by omitting the primary antibody^[15].

Preparation for transmission electron microscopy examination

Pancreas specimens were finely cut into teeny sections that were immediately fixed in 4% phosphate-buffered glutaraldehyde (0.1 mol/L, pH 7.4), at 4°C for 24 hours. Sections were post-fixed in isotonic 1% osmium tetroxide for 1h and were dehydrated in serial dilutions of ethanol. Then, sections were immersed in propylene oxide then were embedded in epoxy resin mixture. Later, semithin sections (1µm thickness) were cut and stained with 1% toluidine blue to be examined by light microscope, while ultrathin sections (80-90nm thickness) were double stained with uranyl acetate and lead citrate to be examined and photographed at different magnification by JEOL-JEM-100 transmission electron microscope (Tokyo, Japan) in Tanta E.M Center, Faculty of Medicine, Tanta University^[16].

Morphometric analysis

A light microscope (Leica DM500, Switzerland) connected to a digital camera (Leica ICC50, Switzerland) was used to obtain images. For morphometric analysis, the software "ImageJ" (version 1.48v National Institute of Health, Bethesda, Maryland, USA) was used. Ten non-overlapping randomly selected fields for each slide in each group were examined at a magnification of 400 to quantitatively evaluate:

1. The mean area percentage of the collagen fibers content in Masson's Trichrome-stained sections^[17].
2. The mean area percentage of VEGF using VEGF immune-stained sections^[18].
3. The mean of zymogen granules count in toluidine blue stained sections^[19].

Statistical analysis

The morphometric results were analyzed using one-way analysis of variance (ANOVA) followed by the Tuckey post hoc test using GraphPad Prism 7.0 (GraphPad Software, Inc.). Data were displayed as means ± standard deviation (SD). Differences were regarded as statistically significant if the probability value $p < 0.05$ and extremely significant if $p < 0.001$, while $p > 0.05$ was considered statistically insignificant^[20].

RESULTS

In the present work, no mortality was recorded during

the experimental period. All subgroups of the control group showed no variance in the histological results. So, it was referred to subgroups (Ia, Ib, Ic) as the control group. Moreover, group II (GE-group) showed no difference in the histological results or the statistical analysis of the morphometric data when compared to the control group.

Light Microscopic Examination

Histological Results

Hematoxylin & Eosin (H&E) stained sections

Group I (Control group) and **group II** (GE-group): Examination of H&E stained pancreatic sections of the control group and GE-group showed the known histological structure of the normal pancreas. Pancreatic lobules were separated by thin connective tissue septae. Each lobule consisted of closely packed exocrine acini lined by pyramidal cells with basal basophilia and apical acidophilia. Acinar cells had basal rounded vesicular nuclei with prominent nucleoli, some of them had double nuclei. The nuclei of centroacinar cells were seen inside the lumen of some acini. Islets of Langerhans appeared as pale oval areas in between the dark acini. Moreover, intralobular ducts lined by cubical cells and normal blood capillaries were also seen (Figures 1 A,B).

Group III (TZ-group): H&E stained sections of the TZ-group showed loss of the normal pancreatic architecture and distorted acini with peri-nuclear haloes surrounding the nuclei of many acinar cells as well as deposition of fibers in between the acini (Figure 1C). Wide separation between the lobules with extravasation of blood into the interlobular spaces (Figure 1D), together with dilated congested intralobular and interlobular blood vessels as well as congested blood capillaries (Figure 1E) were noticed. Moreover, a dilated pancreatic duct with retained acidophilic secretion in its lumen and inflammatory cellular infiltration were also observed (Figure 1F). The acini showed vacuolated cytoplasm with loss of the characteristic basal basophilia (Figure 1G). Furthermore, most acinar nuclei were surrounded by peri-nuclear haloes and some of them appeared pyknotic (Figure 1H).

Group IV (TZ&GE-group): H&E stained sections of the TZ&GE-group showed almost normal architecture of the pancreatic tissue. Pancreatic lobules were separated by thin connective tissue septae and contained closely packed exocrine acini having basal basophilia and apical acidophilia. Intralobular ducts lined by cubical cells and normal blood capillaries were seen in between the acini. Most acini appeared normal with rounded vesicular nuclei or double nuclei. However, there were few destructed acini, and some acinar nuclei were surrounded by peri-nuclear haloes (Figures 1 I,J).

Masson's trichrome stained sections

Few and fine collagen fibers were seen around the ducts, in between the acini, and around the blood capillaries in the control and GE groups (Figure 2A). Marked

deposition of collagen fibers around the blood vessels and ducts, and in between the lobules were observed in the TZ-group (Figures 2 B,C), whereas the TZ&GE-group showed moderate deposition of collagen fibers around the blood vessels and in between the lobules as well as mild deposition of collagen fibers around the blood capillaries (Figure 2D).

Toluidine blue (Tb) stained sections

Examination of Tb-stained pancreatic sections of both control and GE groups showed acinar cells with vesicular nuclei and numerous zymogen granules in their apical part. Nuclei of centroacinar cells were seen inside the lumen of some acini (Figure 3A). TZ-group (group III) showed cytoplasmic vacuoles and few apical zymogen granules in most of the pancreatic acinar cells (Figure 3B). TZ&GE-group (group IV) showed almost normal pancreatic acini had acinar cells with vesicular nuclei and numerous zymogen granules in their apical part (Figure 3C).

Immunohistochemical Results

VEGF immunostained sections of the control group and GE-group revealed localized weak positive cytoplasmic immunoreaction in the cells lining the walls of blood vessels (Figure 4A). On the other hand, a strong positive cytoplasmic immunoreaction was seen in the cells lining the walls of blood vessels and blood capillaries in the TZ-group (Figures 4 B,C). The TZ&GE-group revealed localized weak positive cytoplasmic immunoreaction in the cells lining the walls of blood vessels (Figure 4D).

Morphometric Results

In the present study, no significant statistical differences were noticed in the morphometric and statistical analysis between the control group (group I) and the GE-group (group II). On the other hand, there was an extremely significant increase ($p < 0.001$) in the mean area percentage of collagen and VEGF (30.773 ± 4.04 ; 9.065 ± 1.929 respectively), and an extremely significant decrease ($p < 0.001$) in the mean of zymogen granules count (2105.27 ± 593.41) in TZ-group (group III) versus the control group (9.021 ± 1.36 ; 0.599 ± 0.457 ; 6130.84 ± 632.15 for area % of collagen & VEGF and zymogen granules count respectively). However, there was an extremely significant decrease ($p < 0.001$) in the mean area percentage of collagen fibers and VEGF (9.76 ± 1.24 ; 0.896 ± 0.574 respectively) and an extremely significant increase ($p < 0.001$) in the

mean number of zymogen granules (5903.69 ± 658.27) in TZ&GE-group versus the TZ-group (group III). Moreover, there was a non-significant difference ($p > 0.05$) in the TZ & GE-group versus the control group (group I) in all values of the morphometric analysis (Table1; Histograms 1,2,3).

Electron Microscopic Examination

Group I (Control group) and **group II** (GE-group): Ultrathin sections of the pancreas of both control and GE groups revealed acinar cells with apical numerous electron-dense zymogen granules, normal rER, and mitochondria as well as regular basal rounded nuclei (Figure 5A). Regular intact junctional complexes were noticed between the acinar cells as well as microvilli (Figure 5B) and normal centroacinar cells (Figure 5C) were seen in the acinar lumen. In addition, intralobular ducts lined by intact cubical cells appeared in between the acini (Figure 5D).

Group III (TZ-group): Ultrathin sections of the pancreas of TZ-group revealed acinar cells with cytoplasmic vacuolations, dilated rER, and zymogen granules with different densities as well as irregular dark nuclei with dilated perinuclear space (Figure 6A). Some acinar cells showed dilation of the perinuclear space and heterogeneous electron-dense structures most probably heterolysosomes (Figure 6B). Other acinar cells exhibited zymogen granules with clumping of their contents in their cores (Figure 6C). Moreover, deformed irregular intercellular junctions were noticed between some acinar cells (Figure 6D), and centroacinar cells with irregular indented nuclei were observed in the lumen of some acini (Figure 6E). Meanwhile, the interstitial tissue showed deposition of collagen fibers, and inflammatory cellular infiltration included mast cells (Figure 6F). Furthermore, some intralobular ducts with indented and deformed nuclei appeared in between the acini (Figure 6G).

Group IV (TZ & GE-group): Ultrathin sections of the pancreas of TZ & GE-group revealed nearly normal acinar cells with apical numerous electron-dense zymogen granules, normal rER, and basal rounded euchromatic nuclei (Figure 7A). Few acinar cells showed clumping of zymogen granules' contents in their cores and mild nuclear indentation (Figure 7B). Moreover, few cytoplasmic vacuoles were occasionally noticed in some acinar cells with normal centroacinar cells in the acinar lumen (Figure 7C). Normal regular junctional complexes were observed in between the acinar cells (Figure 7D).

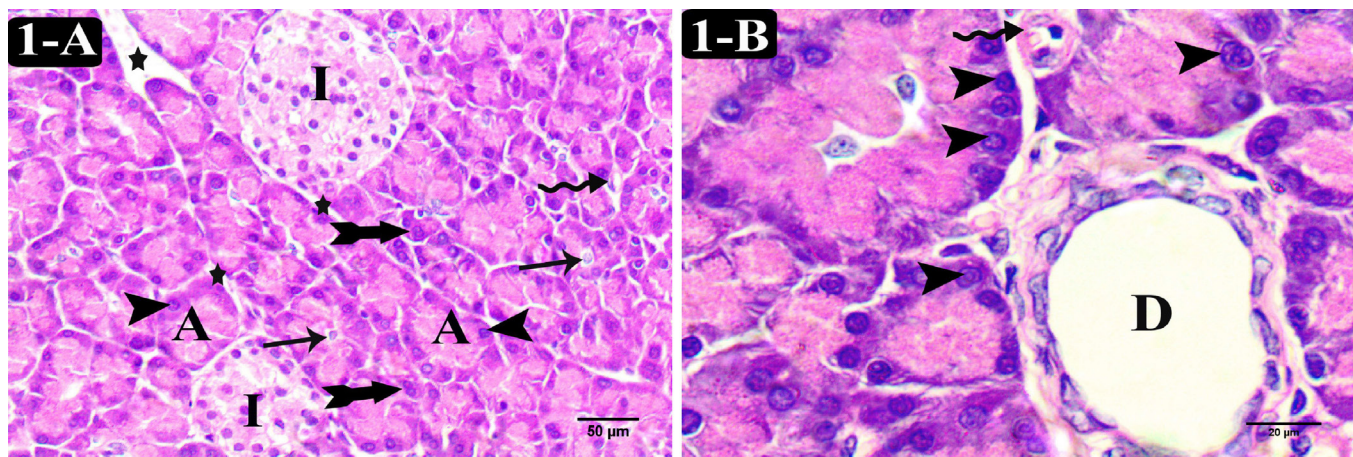


Fig. 1 A&B: Photomicrographs of H&E-stained pancreatic sections from the control group. (A): shows pancreatic lobules are separated by thin connective tissue septae (stars). Each lobule consists of closely packed exocrine acini (A) that are lined by pyramidal cells with basal basophilia and apical acidophilia and have basal rounded vesicular nuclei (arrowheads). Some acinar cells have double nuclei (bifid arrows). The nuclei of centroacinar cells are seen inside the lumen of some acini (thin arrows) and islets of Langerhans (I) appear as pale oval areas in between the dark acini. Notice a normal blood capillary (wavy arrow) (x 400, scale bar = 50 μ m). (B): shows acinar cells have basal, rounded nuclei with prominent nucleoli (arrowheads). An intralobular duct (D) lined by cubical cells is seen in between the acini. Notice a normal blood capillary (wavy arrow) (x 1000, scale bar = 20 μ m).

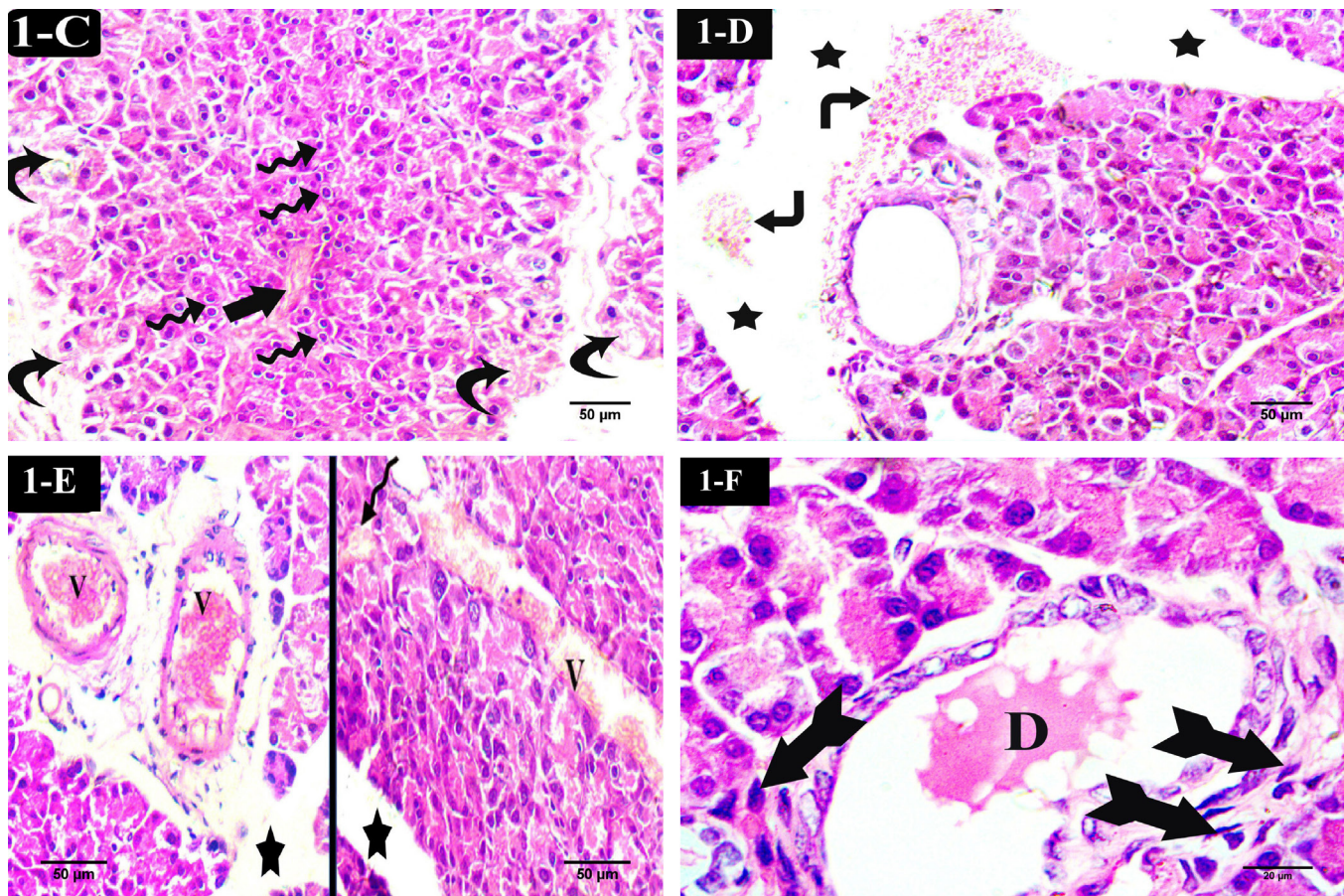


Fig. 1 C, D, E & F: Photomicrographs of H&E-stained pancreatic sections from the TZ-group. (C) shows loss of the normal pancreatic architecture with distorted acini (curved arrows) and peri-nuclear haloes around the nuclei of many acinar cells (wavy arrows). Notice the deposition of fibers in between the acini (thick arrow) (x 400, scale bar = 50 μ m). (D): shows a wide separation between pancreatic lobules (stars) with extravasation of blood into the interlobular spaces (arched arrows) (x 400, scale bar = 50 μ m). (E): shows dilated congested intralobular and interlobular blood vessels (V) as well as a congested blood capillary (wavy arrow). Notice the wide separation between lobules (stars) (x 400, scale bar = 50 μ m). (F): shows a dilated pancreatic duct (D) containing retained acidophilic secretion. Notice the inflammatory cellular infiltration (bifid arrows) (x 1000, scale bar = 20 μ m).

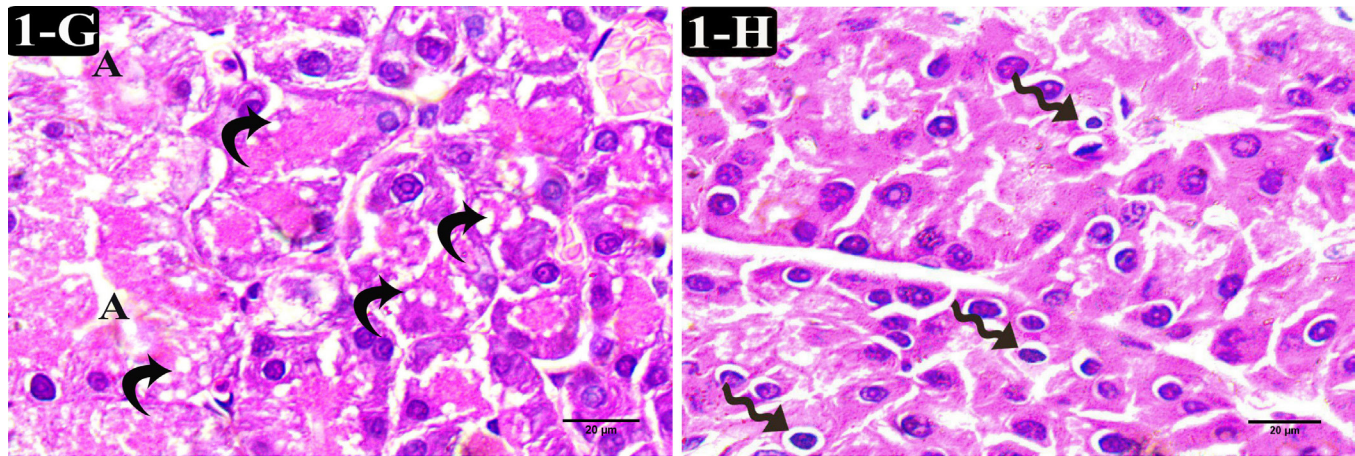


Fig. 1 G & H: Photomicrographs of H&E-stained pancreatic sections from the TZ-group. (G): shows distorted acini with vacuolated cytoplasm (curved arrows) and loss of the characteristic basal basophilia (A) (x 1000, scale bar = 20 µm). (H): shows most acinar nuclei are surrounded by peri-nuclear haloes and some nuclei appear pyknotic (wavy arrows) (x 1000, scale bar = 20 µm).

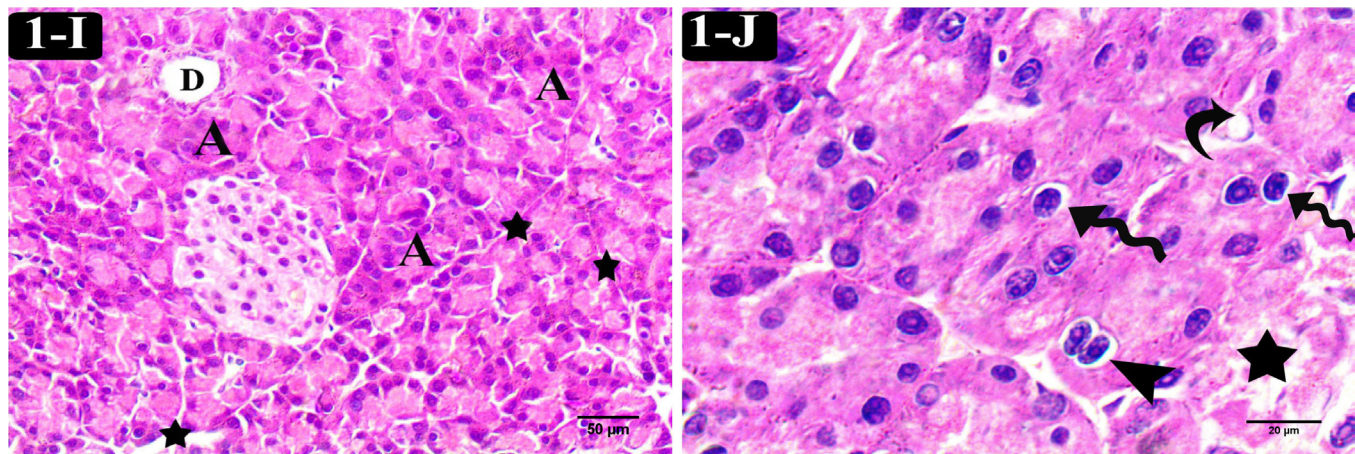


Fig. 1 I & J: Photomicrographs of H&E-stained pancreatic sections from the TZ & GE-group. (I): shows an almost normal architecture of pancreatic tissue as pancreatic lobules are separated by thin connective tissue septae (stars) and contain closely packed exocrine acini (A) which have basal basophilia and apical acidophilia. Notice an intralobular duct (D) lined by cubical cells is seen in between the acini (x 400, scale bar = 50 µm). (J): shows nearly normal acini but few acinar nuclei are surrounded by peri-nuclear haloes (wavy arrows) and some acinar cells have double nuclei (arrowhead). Notice a normal blood capillary (curved arrow) and few destructed acini (star) (x 1000, scale bar = 20 µm).

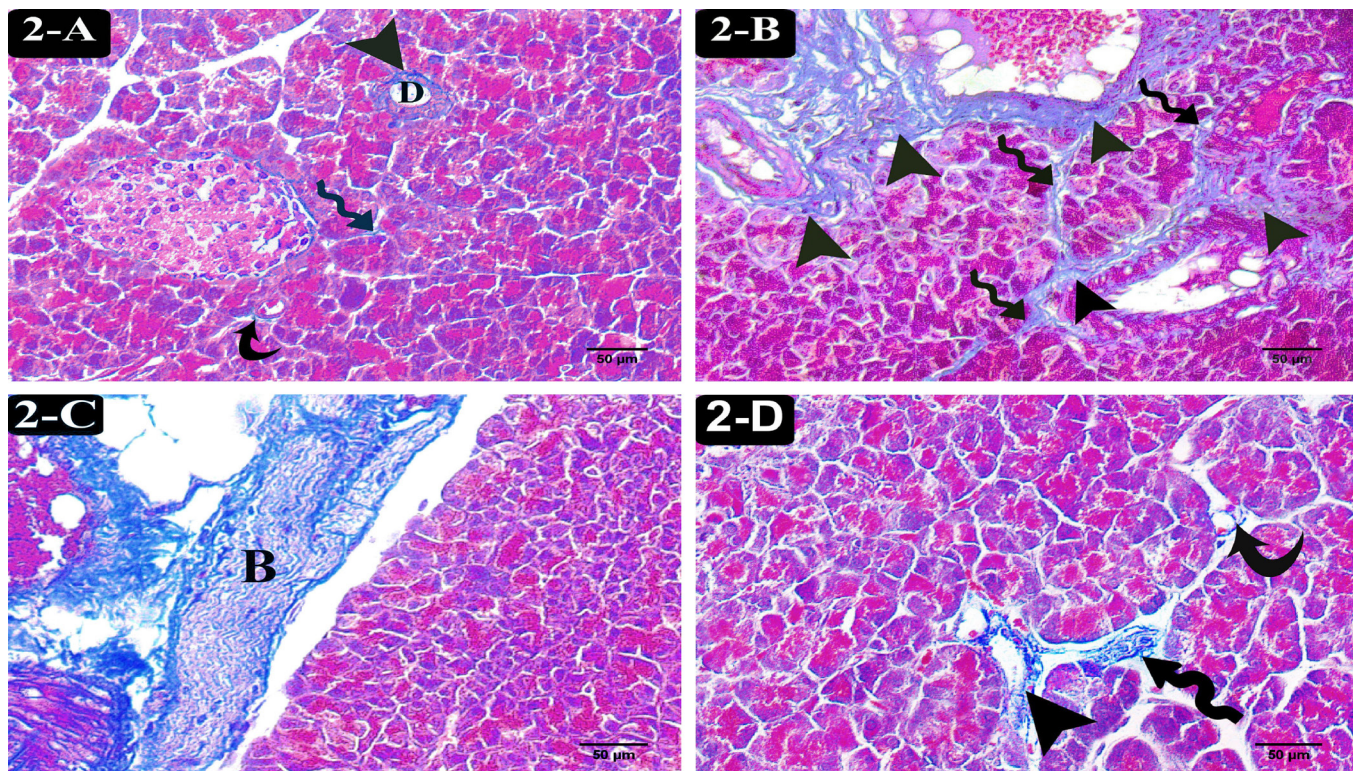


Fig. 2 A, B, C & D: Photomicrographs of Masson's Trichrome stained pancreatic sections. (A): The control group shows few fine collagen fibers (arrowhead) around the ducts (D), in between the acini (wavy arrow), and around the blood capillaries (curved arrow). (B): The TZ group shows marked deposition of collagen fibers around the blood vessels and ducts (arrowheads) and in between the lobules (wavy arrows). (C): The TZ-group shows deposition of collagen bundles (B) in the interlobular tissue. (D): The TZ&GE-group shows moderate deposition of collagen fibers around the blood vessels (arrowhead) and in between the lobules (wavy arrow) as well as mild deposition of collagen around the blood capillaries (curved arrow). (x 400, scale bar = 50 µm)

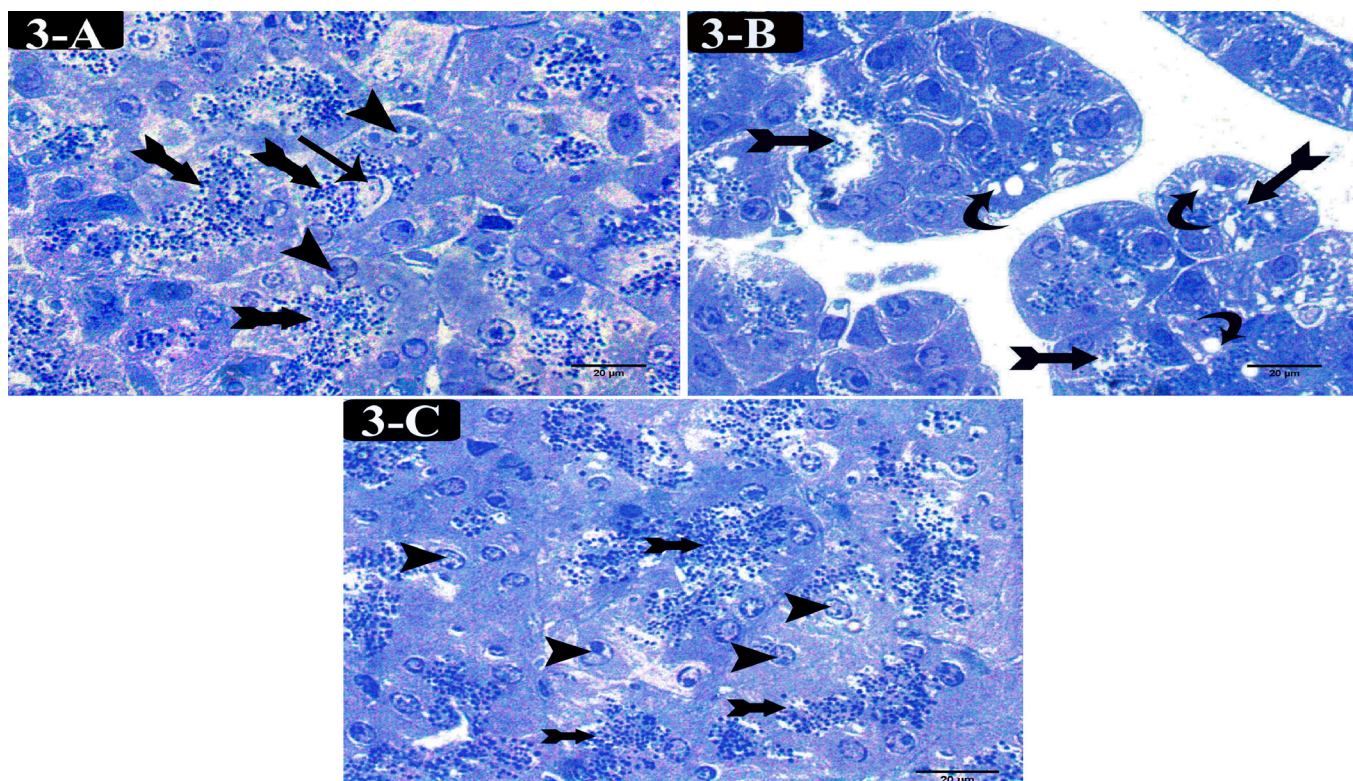


Fig. 3 A, B & C: Photomicrograph of Toluidine blue stained pancreatic sections. (A): The control group shows acinar cells with vesicular nuclei (arrowheads) and numerous zymogen granules in their apical part (bifid arrows). Notice the nuclei of centroacinar cells are seen inside the lumen of some acini (thin arrow). (B): The TZ-group shows cytoplasmic vacuoles (curved arrows) and few apical zymogen granules (bifid arrows) in most of the pancreatic acinar cells. (C): The TZ & GE-group shows almost normal pancreatic acini are lined by acinar cells with vesicular nuclei (arrowheads) and numerous zymogen granules (bifid arrows) in their apical part. (x1000, scale bar = 20 µm)

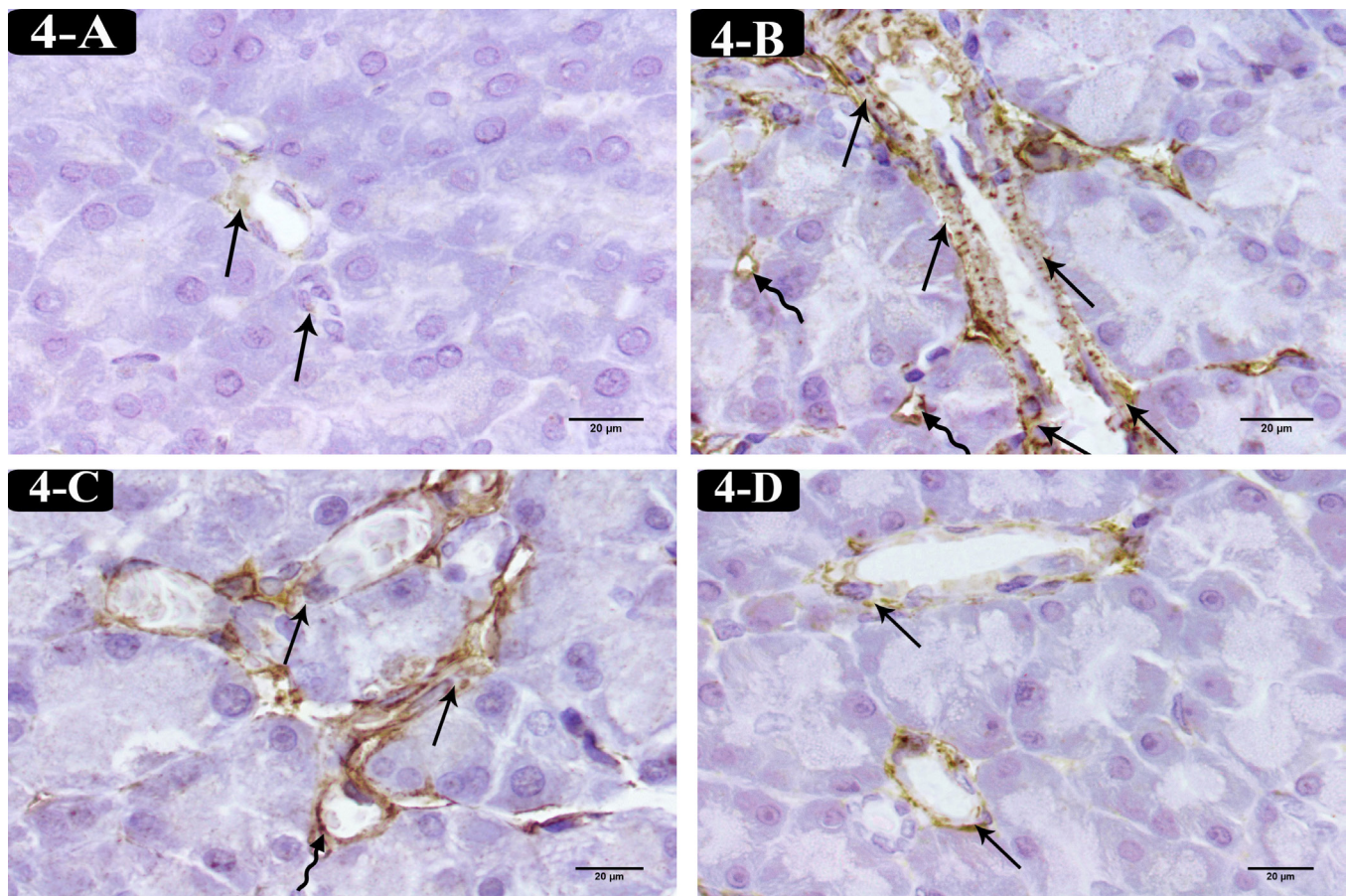


Fig. 4 A, B, C & D: Photomicrographs of VEGF immune-stained pancreatic sections. (A): The control group shows localized weak positive cytoplasmic immunoreaction in the cells lining the walls of blood vessels (thin arrows). (B&C): The TZ-group shows strong positive cytoplasmic immunoreaction in the cells lining the walls of blood vessels (thin arrows) and blood capillaries (wavy arrows). (D): The TZ & GE-group shows localized weak positive cytoplasmic immunoreaction in the cells lining the walls of blood vessels (thin arrows). (x 1000, scale bar = 20 µm)

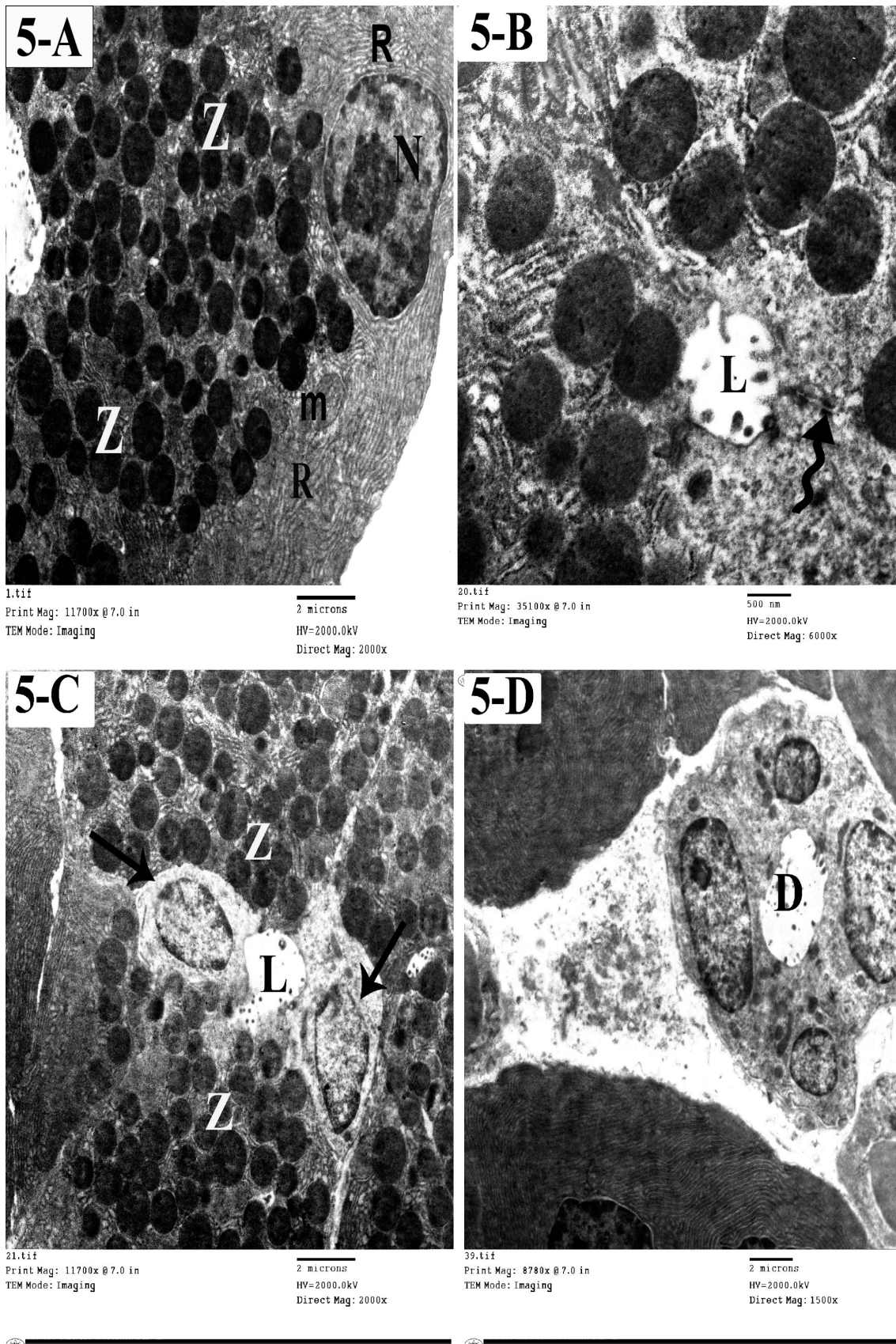


Fig. 5 A, B, C & D: Electron micrographs of ultrathin pancreatic sections from the control group. (A): shows an acinar cell has a basal rounded nucleus (N) and apical numerous electron-dense zymogen granules (Z). Notice normal rER (R) and mitochondria (m) (X 2000). (B): shows a lumen (L) of an acinus containing microvilli. Notice the regular intact junctional complexes (wavy arrow) in between the acinar cells (X 6000). (C): shows a lumen (L) of an acinus containing microvilli and centroacinar cells (arrows). Notice numerous electron-dense zymogen granules (Z) (X 2000). (D): shows an intralobular duct (D) lined by cubical cells (X 1500).

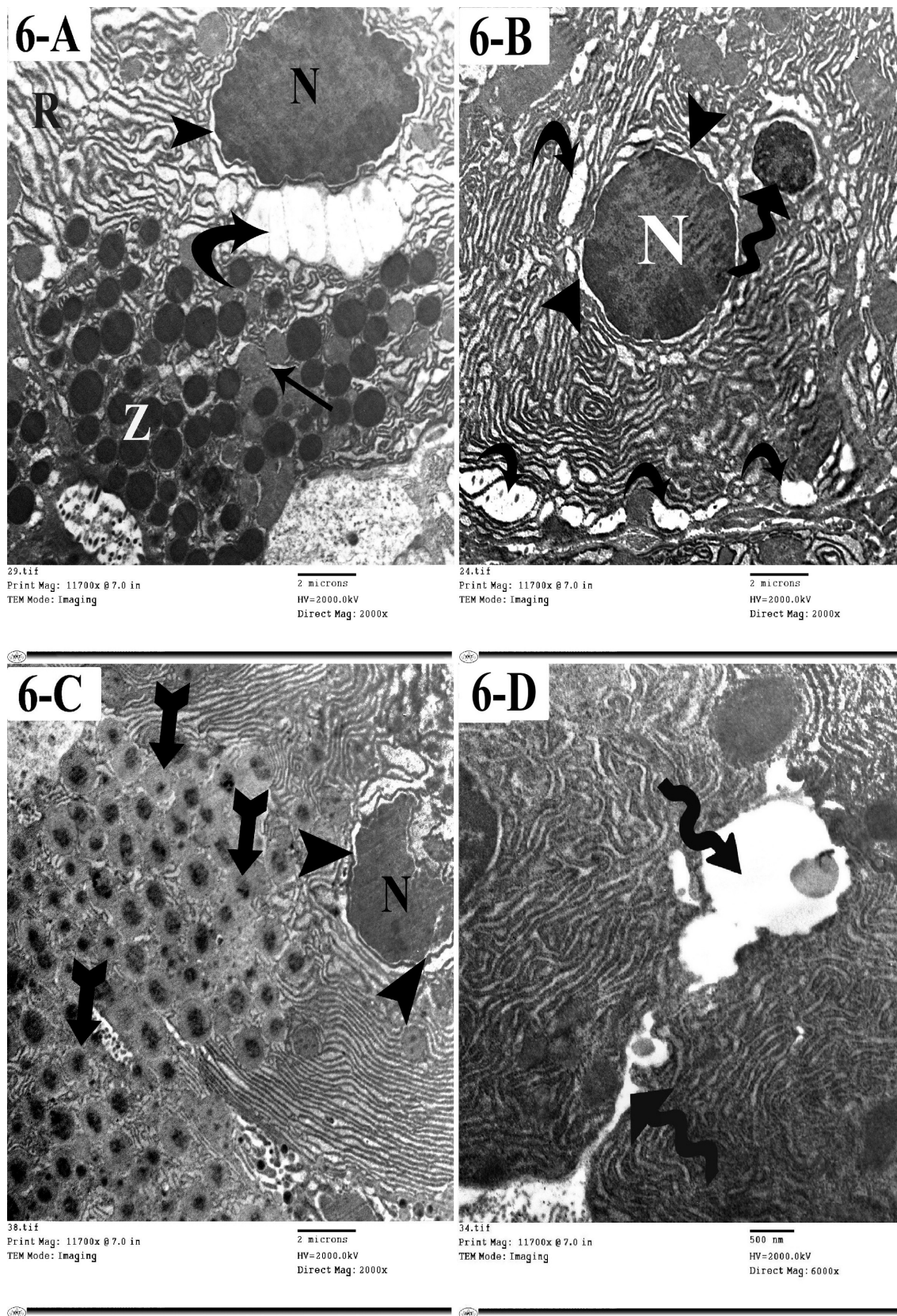


Fig.6- A, B, C & D: Electron micrographs of ultrathin pancreatic sections from the TZ-group. (A): shows an acinar cell exhibits an irregular dark nucleus (N) with dilated perinuclear space (arrowhead), dilated rER (R), vacuolated cytoplasm (curved arrow), and Zymogen granules (Z) with different densities as some of them appear less electron-dense (arrow) (X 2000). (B): shows an acinar cell has a nucleus (N) with dilated perinuclear space (arrowheads), dilated rER cisternae (curved arrows), and unobservable zymogen granules. Notice a heterogeneous electron-dense structure most probably a heterolysosome (wavy arrow) (X 2000). (C): shows zymogen granules alterations manifesting as clumping of their contents in their cores (bifid arrows). Notice the dark irregular nucleus (N) with dilated peri-nuclear space (arrowheads) (X 2000). (D): shows deformed junctional complexes (wavy arrows) between the acinar cells (X 6000).

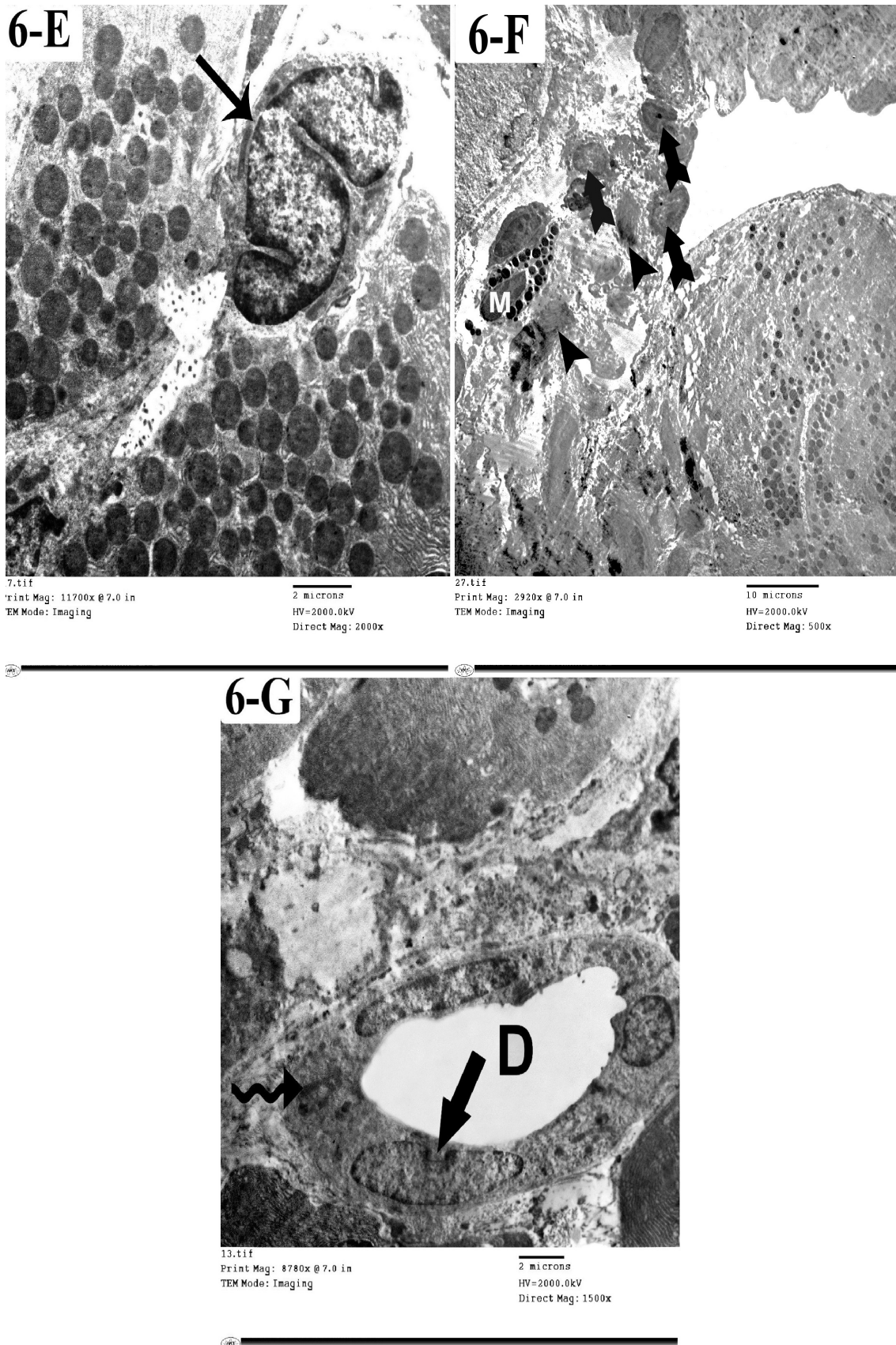


Fig.6- E, F & G: Electron micrographs of ultrathin pancreatic sections from the TZ-group. (E): shows a markedly indented nucleus of a centroacinar cell (arrow) (X 2000). (F): shows interstitial inflammatory cellular infiltration (bifid arrows) including a mast cell (M). Notice collagen fibers (arrowheads) (X 500). (G): shows an intralobular duct (D) with indented (thick arrow) and deformed (wavy arrow) nuclei in their lining epithelium (X 1500).

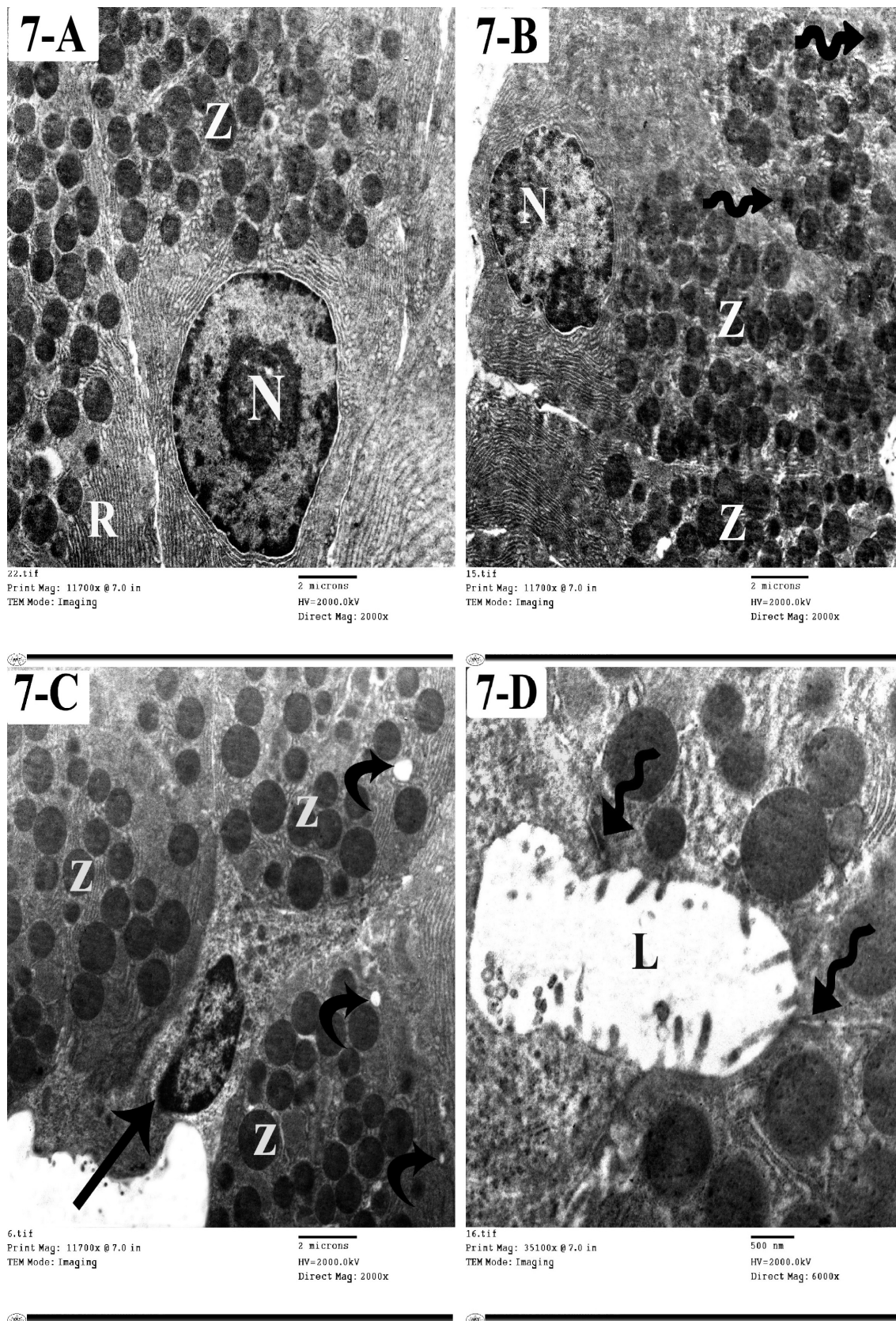
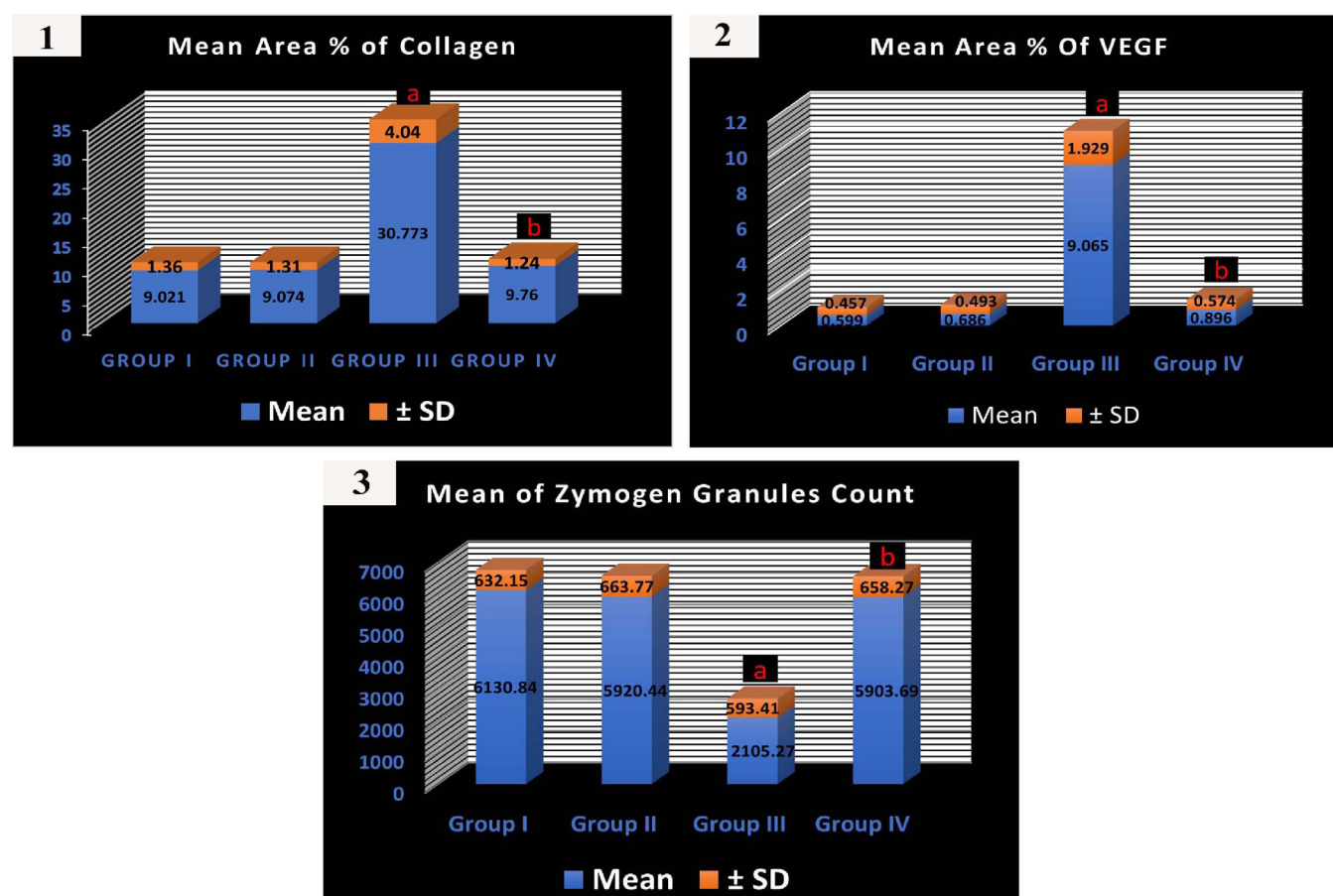


Fig.7- A, B, C & D: Electron micrograph of ultrathin pancreatic sections from the TZ&GE-group. (A) shows an acinar cell has a basal rounded nucleus (N), apical numerous electron-dense zymogen granules (Z) & normal rER (R) (X 2000). (B): shows an acinar cell with a basal mild indented nucleus (N), apical numerous electron-dense zymogen granules (Z), some of them appear with clumping of their contents in their cores (wavy arrows) (X 2000). (C): shows more or less normal acinar cells with apical numerous electron-dense zymogen granules (Z), and a normal centroacinar cell (thin arrow). Notice few cytoplasmic vacuoles (curved arrow) in the acinar cells (X 2000). (D): shows a lumen (L) of an acinus containing microvilli. Notice normal regular junctional complexes (wavy arrow) in between the acinar cells (X 6000).



Histograms 1: shows the mean \pm SD of the mean area percentage of collagen fibers in all studied groups. (2) shows the mean \pm SD of the area percentage of VEGF in all studied groups. (3) shows the mean \pm SD of zymogen granules count in all studied groups. (a indicates a highly significant versus control and b indicates a highly significant versus group III)

DISCUSSION

The reckless use of food coloring dyes in our daily food and non-food items obliges us to investigate their harmful effects on different organs in our bodies. Tartrazine is now one of the most widely used food coloring and food additives materials^[6]. Moreover, tartrazine is found not only in food products but also in children's toys and accessories which could expose the children to excess tartrazine by different routes than food^[21].

Tartrazine can induce oxidative stress by overproduction of ROS which causes cellular dysfunction and affects all cellular components such as lipids, proteins, nucleic acids, and carbohydrates. That oxidative stress is a leading cause in the pathogenesis of numerous diseases including acute and chronic pancreatitis as reported by Ameer *et al.*^[21] and Leung and Chan^[22] Moreover, the toxic effects of tartrazine on the pancreatic tissue may be performed by its major metabolite as the byproduct's metabolism can be more toxic than its precursor from which they are derived^[23]. As the anti-oxidative system in the pancreatic tissue is so weak and less powerful than other tissues, so the pancreas is more sensitive to the oxidative stress and requires more antioxidant support^[8]. So, we aimed in the present study to demonstrate the histopathological changes in the exocrine portion of the pancreas of albino rats treated with tartrazine

and to assess the possible ameliorating effects of geraniol against tartrazine-induced hazards.

The disturbed architecture of acinar cells in the TZ-group can be attributed to tartrazine-induced oxidative damage and peroxidation of lipids in the acinar cell membranes, which in turn impact the cellular activities through changing the cell membranes' integrity, fluidity, and physicochemical features with subsequent lipid peroxidation and cell death^[6,24].

The vacuolated cytoplasm in the pancreatic acinar cells in the TZ-group is consistence with the histological findings of many investigators such as Ghonimi and Elbaz^[25], El-Sakhawy *et al.*^[26], and Wu *et al.*^[27] who observed cytoplasmic vacuolation of the acinar cells in the submandibular gland, epithelial cells in the intestine, and in the hepatocytes as well as in the cerebellar neurons in rats exposed to tartrazine. They attributed this finding to tartrazine toxicity and explained that cytoplasmic vacuolation is a sign of cell apoptosis as cells compensate by vacuolating and swelling. They added that the vacuolar degeneration in tartrazine-treated animals might be caused by loss of the cell membrane's selective permeability with subsequent disturbance in the intracellular fluid and electrolytes which in turn caused dilatation of the cytoplasmic components which is the first sign of cell injury. Also, Miller and

Zachary^[28] explained that these cytoplasmic vacuolations might be a cellular defense mechanism against injurious substances. However, another explanation was reported by Yasser and Shon^[29] that cytoplasmic vacuolation could be a sequence of the accumulation of lipid which was dissolved through the fixation and tissue processing.

Regarding the loss of characteristic basal cytoplasmic basophilia in the TZ-group, this finding could be explained according to Priyadi *et al.*^[30] to be due to rER depletion. Moreover, the depletion of zymogen granules that were noticed in TB stained sections in the TZ-group and was confirmed by the statistical analysis could be attributed according to Yassien and El-ghazouly^[31] to the increment in the process of exocytosis. Also, most acinar nuclei in group III were surrounded by peri-nuclear haloes and some nuclei appeared pyknotic. These findings are correlated with Oyewole and Oladele^[32] who recorded that tartrazine caused deformities and irregularity in the shapes and sizes of the nuclei of the cardiomyocytes. According to El Shahawy and El Deeb^[33], these nuclear changes are considered a sign of cellular degeneration, apoptosis, and cell death.

Moreover, the wide separation between pancreatic lobules is in accordance with the findings of many researchers; Abdel-Aziz *et al.*^[12] within the thyroid glands of TZ-treated rats, Haroun *et al.*^[34] in rats had acute pancreatitis induced by energy drinks as well as Yassien and El-ghazouly^[31] in atorvastatin induced acute pancreatitis. They explained that edema might be the cause of the widening of the interlobular and interacinar septae and they attributed edema to high endogenous nitric oxide that increased the permeability of blood vessels.

Further, inflammatory cellular infiltration was noticed in the TZ-group and was confirmed by electron microscopic examination which revealed interstitial inflammatory cells including mast cells. This was previously noticed in a recent study done by Kandeel and Sharaf Eldin^[35], who observed marked inflammatory cellular infiltrations in the lamina propria of the jejunal mucosa of tartrazine-treated rats. They explained that TZ promotes a pro-inflammatory response by triggering the inflammatory cells in tissues and by the synthesis of leukotrienes. Previous research by Lopez-Font *et al.*^[36] reported that mast cells play an important role in the inflammatory response by increasing vascular permeability and leukocyte accumulation.

Dilated congested pancreatic blood vessels accompanied by extravasations of blood cells into the surrounding interstitial tissue in the TZ-group agree with the findings of El-Desoky *et al.*^[37] who noticed dilated congested blood sinusoids and central veins with interstitial hemorrhage in the liver of TZ-treated rats as well as dilated congested glomerular capillaries with interstitial hemorrhage in the renal tissue in the same group. Some authors as El-Sakhawy *et al.*^[26] and Moubarak^[38] explained that congestion and interstitial hemorrhage are considered an inflammatory response to get more blood to the regions

of degeneration and that congestion causes an increment in the capillary hydrostatic pressure which increases the capillary permeability in the site of inflammation that in turn can cause edema.

In this study, some ducts in the TZ-group were dilated and contained retained secretion. This is in accordance with El-Sakhawy *et al.*^[26] who noticed severed degenerative changes and sloughing of the epithelial lining of striated ducts of submandibular glands of TZ-treated rats. They attributed these findings to a defect in the cellular metabolism which in turn caused a morphological disturbance with subsequent loss of normal architecture, while stagnant secretion might be due to depletion of ATP with a subsequent disorder in biosynthesis and membrane pumps, so cells lack the energy needed for transportation of their secretion. Contrary to our results, a study done by Ameer *et al.*^[23] recorded that the pancreatic duct and interlobular ducts in tartrazine-treated rats appeared almost normal without any pathological changes.

Furthermore, Masson's trichrome stained sections revealed a significant increase in the collagen deposition in the TZ-group mainly around the blood vessels, ducts, and in between the lobules. This was confirmed by the statistical analysis of the area percentage of collagen deposition. This result agrees with Megahed *et al.*^[39] who noticed in the heart of TZ-treated rats, a marked deposition of collagen fibers in between the cardiomyocytes and around the blood vessels. A previous study by Kandeel and Sharaf Eldin^[35] attributed this finding to TZ-induced oxidative stress which can cause inflammation, cytokine dysregulations, and release of the TNF- α by the damaged tissue with subsequent stimulation of fibroblasts differentiation into fibrocytes, tissue fibrosis and collagen deposition.

Vascular endothelial growth factor (VEGF), which is also called vascular permeability factor, is released by various types of cells such as smooth muscle cells, macrophages, and mast cells. It is a signaling protein that promotes the growth of new blood vessels (angiogenesis), in both normal and pathological circumstances^[40,41]. In the current study, a strong positive VEGF immunoreaction was noticed in the cytoplasm of cells lining the walls of blood vessels and blood capillaries in the pancreatic sections of the tartrazine group which was confirmed by the morphometric study and statistical analysis. This finding was previously noticed by Li *et al.*^[42] in acute pancreatitis and by Sadek and Khattab^[18] in L-arginine-induced acute pancreatitis as well as by Yassien and El-ghazouly^[31] in Atorvastatin induced pancreatitis.

The biological role of VEGF exceeds angiogenesis as VEGF is also a main mediator of wound repair^[43]. It participates in the host inflammatory response in several pathological conditions and inflammatory response mainly in the vascular endothelial cells by binding to Flt-1 which activates neutrophils and promotes neutrophils chemotaxis^[44]. Accordingly, the increased VEGF in the pancreatic tissues of the tartrazine group may be

considered a compensatory mechanism for pancreatitis with subsequent restoration of the pancreas either through the stimulation of the ductal cells' maturation or by new capillaries formation^[18,31,45]. On the other hand, Nandy and Mukhopadhyay^[46] reported that increasing the expression of the VEGF is limited only to the malignant transformation of the pancreas, not to pancreatitis.

Electron microscopic examination revealed heterogeneous electron-dense structures most probably heterolysosomes and dilated cisternae of rER in the TZ-group, which were also observed by Khayyat *et al.*^[47] in the liver and kidney of tartrazine-treated rats. They attributed that to be a response to chemical stressors and the toxic effect of tartrazine. Also, Soliman^[48] reported that oxidative stress causes endoplasmic reticulum (ER) stress with subsequent severe ER dilatation. Moreover, Ali *et al.*^[49] confirmed that the endoplasmic reticulum is highly exposed to free radicals, as it is considered a radical generating site and its membranes are full of polyunsaturated fatty acids that are sensitive to free radical attack. Yassien and El-ghazouly^[31] reported that rER dilatation is a sign of elevated protein formation as a compensatory mechanism to zymogen granules depletion that can be attributed to increasing exocytosis.

The alterations that were noticed in zymogen granules in the TZ-group were interpreted by Schmidt *et al.*^[50] as a defect in the synthesis of the sub-membranous matrix causing a failure of the granular content to adhere to the surrounding membrane. Also, Ostapenko *et al.*^[51] explained that the variation in zymogenic granules' size and electron density revealed different degrees of ripening of the secretory products. Moreover, Sah *et al.*^[52] stated that pancreatitis causes premature intrapancreatic trypsinogen activation, which leads to dysregulation of digestive enzyme synthesis and secretion.

The deformities and irregularities in the junctional complexes with subsequent widening of the intercellular space that were noticed in TZ-group in the present study are in accordance with the findings of Megahed *et al.*^[39] in the heart of TZ-treated rats as cardiomyocytes were separated from each other by wide intercellular spaces. Also, Abonar *et al.*^[53] observed that acinar cells in pancreatitis became isolated from one another when fluid leaked into the intercellular spaces. They explained that during the cell injury process, there was a breakdown of the cellular junctions secondary to disturbance of the cytoskeletal filaments as well as suppression of making of the junctional adhesion molecules with subsequent separation of the adjacent cells from each other.

Regarding the centroacinar cells in the TZ-group, some of them revealed irregular indented nuclei which according to Rovira *et al.*^[54] and Delaspre *et al.*^[55] could be a clue to the occurrence of defects in pancreatic homeostasis as centroacinar cells act as progenitor cells and play an important role in keeping tissue homeostasis, so they have an essential function in the treatment of various pancreatic diseases.

Geraniol is a substantial component in the essential oils of ginger, lemon, lime, orange, and nutmeg. Recently, it attracted great interest due to its various biological and pharmacological characteristics^[56]. In this study, geraniol coadministration with tartrazine in group IV (TZ & GE- group) markedly improved the pancreatic tissues and showed an almost normal pancreatic architecture with increased zymogen granules in number and density and decreased the inflammatory cellular infiltration and collagen deposition compared to tartrazine group. This protective effect of geraniol on the histological structure of the pancreatic tissues may be attributed to the anti-inflammatory and antioxidant activity of geraniol which showed significant cytoprotective and antioxidant properties against induced oxidative stress^[57].

Normal pancreatic acini were noticed in group IV but occasionally, few vacuolated acinar cells and some dilated cisterns of the rER were seen. This is aligned with Stawiarska-Pięta *et al.*^[58] who reported that the administration of antioxidants causes an increment in the protein and zymogen granules associated with either minimal or non-dilatation of the rER cisternae. Also, this is in accordance with Hosseini *et al.*^[10] and Marcuzzi *et al.*^[59], who explained that geraniol can significantly improve and reduce ROS which is beneficial in treating or preventing oxidative stress, and that geraniol performs its anti-inflammatory effects via decreasing the inflammatory mediators both in *vivo* and in *vitro* thus it can prevent the development of acute pancreatitis. Furthermore, Eskandari *et al.*^[60] reported that treatment of rats with geraniol reduced the level of lipid peroxidation and increased the activity of SOD and GPx enzymes in different tissues (liver, pancreas, and heart tissues).

The morphometric results in the present work confirmed that geraniol could prevent TZ-induced collagen accumulation, as statistical analysis revealed a significant decrease in the area percentage of collagen fibers content in the TZ&GE-group compared to the TZ-group. Agreed with our results, Elguindy *et al.*^[61] observed that geraniol prevented liver fibrosis and caused a significant reduction in the liver fibrosis markers. They also explained that geraniol's anti-inflammatory activity might be one of the pathways that caused its anti-fibrotic effect. Moreover, Jayachandran *et al.*^[62] reported that antioxidants, in general, attenuate fibrosis and that geraniol can effectively inhibit collagen up-regulation.

Also, morphometric results demonstrated an ameliorating effect of geraniol on VEGF immunoeexpression, as statistical analysis revealed a significant decrease in the area percentage of VEGF in the TZ&GE-group compared to the TZ-group. This goes in harmony with Wittig *et al.*^[63] who recorded that geraniol inhibited angiogenesis by blocking signaling pathways for the vascular endothelial growth factor (VEGF).

CONCLUSION AND RECOMMENDATIONS

Based on the above-discussed results, it could be

concluded that tartrazine has adverse effects on the exocrine portion of the pancreas of adult male albino rats and geraniol could ameliorate these toxic effects when given concomitantly with it. Accordingly, it is recommended to raise consumer awareness about the unexpected toxic hazards of tartrazine and to limit the use of such food colorants to preserve public health. Moreover, we recommend labelling the food products that contain tartrazine to limit the consumption of these products, especially in foods and stuff used by children. Further studies are required to demonstrate the molecular pathways by which the food dye tartrazine can induce its toxic effects and to explore the cellular mechanism by which geraniol prevents and/or inhibits these toxic effects.

CONFLICT OF INTERESTS

There are no conflicts of interest.

REFERENCES

1. Rehman K, Ashraf A, Azam F, Akash MS. Effect of food azo-dye tartrazine on physiological functions of pancreas and glucose homeostasis. *Turkish Journal of Biochemistry*. 2019 Apr 1;44(2):197-206. Doi: <https://doi.org/10.1515/tjb-2017-0296>
2. Lahmass I, Sabouni A, Berraouan A, Zoheir K, Belakbir S, Elyoubi M, *et al.* Treatment with saffron extract of the diabetogenic rats induced by the food colorant Tartrazine. *Indian Journal of Physiology and Pharmacology*. 2018; 62(2): 249-58. <https://www.researchgate.net/publication/324692816>
3. Liu B, Zhang H, Cheng X. Exploring the interaction of tartrazine and lipase: a multispectroscopic analysis, docking and computational simulation methods. *Asian Journal of Pharmaceutical Research and Development*. 2019 Aug 14;7(4): 1-7. Doi: <https://doi.org/10.22270/ajprd.v7i4.546>
4. Als Salman N, Aljafari A, Wani TA, Zargar S. High-dose aspirin reverses tartrazine-induced cell growth dysregulation independent of p53 signaling and antioxidant mechanisms in rat brain. *BioMed research international*. 2019 Mar 26;2019. Doi: <https://doi.org/10.1155/2019/9096404>
5. Leulescu M, Rotaru A, Pălărie I, Moanță A, Cioateră N, Popescu M, *et al.* Tartrazine: Physical, thermal and biophysical properties of the most widely employed synthetic yellow food-coloring azo dye. *Journal of Thermal Analysis and Calorimetry*. 2018 Oct;134(1):209-31. Doi:10.1007/s10973-018-7663-3
6. Zafar M, Ali S, Beenish H, Khursheed T, Hussain N, Zakria I. Curcumin's neuroprotective efficacy against tartrazine induced Nissl rim alterations in adult male rats' motor cortex. *Journal of Islamic International Medical College (JIIMC)*. 2021 Sep 1;16 (3):180-4. <https://journals.riphah.edu.pk/index.php/jiimc/article/view/1122>
7. Elekima I, Nwachuku OE, Nduka N, Nwanjo HU, Ukwukwu D. Biochemical and histological changes associated with azo food dye (Tartrazine) in male albino rats. *Asian Journal of Research in Biochemistry*. 2019; 5(1): 1-14. Doi: 10.9734/ajrb/2019/v5i130083
8. Erdemli Z, Altinoz E, Erdemli ME, Gul M, Bag HG, Gul S. Ameliorative effects of crocin on tartrazine dye induced pancreatic adverse effects: a biochemical and histological study. *Environmental Science and Pollution Research*. 2021 Jan;28(2):2209-18. Doi: 10.1007/s11356-020-10578-6
9. Mączka W, Wińska K, Grabarczyk M. One hundred faces of geraniol. *Molecules*. 2020 Jan;25(14):3303. Doi: 10.3390/molecules25143303
10. Hosseini SM, Hejazian LB, Amani R, Siahchrehreh Badeli N. Geraniol attenuates oxidative stress, bioaccumulation, serological and histopathological changes during aluminum chloride-hepatopancreatic toxicity in male Wistar rats. *Environmental Science and Pollution Research*. 2020 March;27(16):20076-20089. Doi: 10.1007/s11356-020-08128-1
11. Younis NS, Abduldaium MS, Mohamed ME. Protective effect of geraniol on oxidative, inflammatory and apoptotic alterations in isoproterenol-induced cardiotoxicity: role of the Keap1/Nrf2/HO-1 and PI3K/Akt/mTOR pathways. *Antioxidants*. 2020 Oct 12;9(10):977. Doi: <https://doi.org/10.3390/antiox9100977>
12. Abdel-Aziz HM, Alazouny ZM, Abdelfadee KF, Abohashem AA. Effect of tartrazine on thyroid gland of male rat and ameliorating role of curcumin (histological and immunohistochemical study). *Journal of Biochemistry and Cell Biology*. 2019;2(111):2-8. Doi: <https://api.semanticscholar.org/CorpusID:212551732>
13. Ghasi S, Umana I, Ogbonna A, Nwokike M, Ufelle S. Cardioprotective effects of animal grade piperazine citrate on isoproterenol-induced myocardial infarction in Wistar rats: biochemical and histopathological evaluation. *African Journal of Pharmacy and Pharmacology*. 2020; 14(8): 285-93. Doi: <https://doi.org/10.5897/AJPP2020.5164>
14. Bancroft J, Layton C. The hematoxylin and eosin, Connective and other mesenchymal tissues with their stains. In: Suvarna S, Layton C and Bancroft J, editors. *Bancroft's Theory and Practice of Histological Techniques*. 8th ed. Elsevier. China. 2019. Chapters 10 and 12. Doi: <https://doi.org/10.1016/C2015-0-00143-5>
15. Buchwalow IB, Böcker W. Working with Antibodies. In: *Immunohistochemistry: Basics and Methods*. Springer Berlin Heidelberg; 2010:31-9. Doi: https://doi.org/10.1007/978-3-642-04609-4_4

16. Zaghloul D, Gad-El-Rab WM, Bushra RR, Farahat AA. The possible protective role of methionine against sodium fluoride-induced pancreatic changes in the adult male albino rat: a histological, immunohistochemical and morphometric study. *Egyptian Journal of Histology*. 2019 Jun 1;42(2):285-96. Doi: 10.21608/EJH.2019.6198.1040
17. Youssef S. Effect of fluoxetine on the pancreas of adult male albino rats and the possible protective role of omega-3: light and electron microscopic study. *International Journal of Clinical and Developmental Anatomy*. 2017;3(6):45-56. Doi: 10.11648/j.ijcda.20170306.11
18. Sadek AS, Khattab RT. The protective role of melatonin on L-arginine-induced acute pancreatitis in adult male albino rats. *Folia morphologica*. 2017; 76 (1) :66-73. Doi: 10.5603/FM.a2016.0029
19. Soliman ME, Kefafy MA, Mansour MA, Ali AF, Ibrahim Esa WA. Histological study on the possible protective effect of pentoxifylline on pancreatic acini of L-arginine-induced acute pancreatitis in adult male albino rats. *Menoufia Medical Journal*. 2014; 27: 801-8. Doi: 10.4103/1110-2098.149789
20. Dawson B, Trapp RG. Basic & Clinical Biostatistics. In: *Basic & Clinical Biostatistics*. 4th ed. Lange Medical Books / McGraw-Hill Medical Publishing Division; 2004:162–89. https://primo.qatar-weill.cornell.edu/permalink/974WCMCIQ_INST/1uk5n69/alma991000014429706691
21. Ameer FZ, Mehedi N, Soler Rivas C, Gonzalez A, Kheroua O, Saidi D. Effect of tartrazine on digestive enzymatic activities: in *vivo* and in *vitro* studies. *Toxicological Research*. 2020 Apr;36(2):159-66. Doi: <https://doi.org/10.1007/s43188-019-00023-3>
22. Leung PS, Chan YC. Role of oxidative stress in pancreatic inflammation. *Antioxidants & redox signaling*. 2009 Jan 1;11(1):135-66. Doi: <https://doi.org/10.1089/ars.2008.2109>
23. Ameer FZ, Mehedi N, Kheroua O, Saïdi D, Salido GM, Gonzalez A. Sulfanilic acid increases intracellular free-calcium concentration, induces reactive oxygen species production and impairs trypsin secretion in pancreatic AR42J cells. *Food and chemical toxicology*. 2018 Oct 1;120: 71-80. Doi:10.1016/j.fct.2018.07.001
24. Al-Daamy AM, Al-Zubiady NM. Study of the toxic effect of tartrazine dye on some biochemical parameters in male albino rats. *Scientific Journal of Medical Research* 2020 Dec 1;4(16):111-7. <https://www.researchgate.net/publication/352030136>
25. Ghonimi WA, Elbaz A. Histological changes of selected Westar rat tissues following the ingestion of tartrazine with special emphasis on the protective effect of royal jelly and cod liver oil. *Journal of Cytology & Histology*. 2015 May 20;6(4):1. Doi:10.4172/2157-7099.1000346
26. El-Sakhawy MA, Mohamed DW, Ahmed YH. Histological and immunohistochemical evaluation of the effect of tartrazine on the cerebellum, submandibular glands, and kidneys of adult male albino rats. *Environmental Science and Pollution Research*. 2019 Apr;26(10):9574-84. Doi:10.1007/s11356-019-04399-5
27. Wu L, Xu Y, Lv X, Chang X, Ma X, Tian X, *et al.* Shi X, Li X, Kong X. Impacts of an azo food dye tartrazine uptake on intestinal barrier, oxidative stress, inflammatory response and intestinal microbiome in crucian carp (*Carassius auratus*). *Ecotoxicology and Environmental Safety*. 2021 Oct 15; 223:112551. Doi: 10.1016/j.ecoenv.2021.112551
28. Miller MA, Zachary JF. Mechanisms and morphology of cellular injury, adaptation, and death. *Pathologic Basis of Veterinary Disease*. 2017 e19;2–43. Doi: 10.1016/B978-0-323-35775-3.00001-1
29. Yasser S, Shon A. Histomorphometric and immunohistochemical study comparing the effect of diabetes mellitus on the acini of the sublingual and submandibular salivary glands of albino rats. *Open Access Macedonian Journal of Medical Sciences*. 2020 Mar 30;8(A):49-54. Doi: <https://doi.org/10.3889/oamjms.2020.3722>
30. Priyadi A, Muhtadi A, Suwantika AA, Sumiwi SA. An economic evaluation of diabetes mellitus management in South-East Asia. *Journal of Advanced Pharmacy Education & Research* | Apr-Jun. 2019;9(2):53-74. <https://japer.in/article/an-economic-evaluation-of-diabetes-mellitus-management-in-south-east-asia>
31. Yassien R, El-ghazouly D. The Effect of atorvastatin on the pancreas of adult male albino rats and the possible protective role of resveratrol (histological, immunohistochemical and biochemical study). *Egyptian Journal of Histology*. 2020 Dec 1;43(4): 1098-1114. Doi: 10.21608/EJH.2020.21365.1218
32. Oyewole OI, Oladele JO. Assessment of cardiac and renal functions in Wistar albino rats administered carmoisine and tartrazine. *Advances in Biochemistry*. 2016 Jul 6;4(3):21-5. Doi: 10.11648/j.ab.20160403.11
33. El Shahawy M, El Deeb M. Assessment of the possible ameliorative effect of curcumin nanoformulation on the submandibular salivary gland of alloxan-induced diabetes in a rat model (Light microscopic and ultrastructural study). *The Saudi Dental Journal*. 2022 Apr 29; 34: 375-384. Doi: <https://doi.org/10.1016/j.sdentj.2022.04.009>
34. Haroun H, Mohamed E, El Shahat AE, Labib H, Atef M. Adverse effects of energy drink on rat pancreas and the therapeutic role of each of bone marrow mesenchymal stem cells and nigella Sativa oil. *Folia Morphologica*. 2020;79(2):272-9. Doi: 10.5603/FM.a2019.0069

35. Kandeel S, EM Sharaf Eldin H. The possible ameliorative effect of manuka honey on tartrazine induced injury of the jejunal mucosa with the role of oxidative stress and TNF-alpha: histological and morphometric study. *Egyptian Journal of Histology*. 2021 Mar 1;44(1): 48-60. Doi: 10.21608/EJH.2020.28580.1280
36. Lopez-Font I, Gea-Sorlí S, de-Madaria E, Gutiérrez LM, Pérez-Mateo M, Closa D. Pancreatic and pulmonary mast cells activation during experimental acute pancreatitis. *World journal of gastroenterology: WJG*. 2010 Jul 7;16(27): 3411-3417. Doi: 10.3748/wjg.v16.i27.3411
37. El-Desoky GE, Abdel-Ghaffar A, Al-Othman ZA, Habila MA, Al-Sheikh YA, Ghneim HK, *et al*. Curcumin protects against tartrazine-mediated oxidative stress and hepatotoxicity in male rats. *European Review for Medical and Pharmacological Sciences*. 2017 Feb 1; 21: 635-45. <https://api.semanticscholar.org/CorpusID:3963241>.
38. Moubarak R. The effect of hypercholesterolemia on the rat parotid salivary gland (histopathological and immunohistochemical study). *Cairo Dental Journal*. 2008;24(1):19-28. <https://api.semanticscholar.org/CorpusID:28779321>.
39. Megahed RM, Barghash SS, Hasan RA. Sub-chronic toxic effects of tartrazine on the heart and brain of adult male albino rats and the protective effect of vitamin E. *Journal of Recent Advances in Medicine*. 2022 Jan 1;3(1):19-30. Doi: <https://doi.org/10.21608/jram.2021.69371.1116>.
40. Neufeld G, Cohen T, Gengrinovitch S, Poltorak Z. Vascular endothelial growth factor (VEGF) and its receptors. *FASEB J*, 1999; 13: 9–2. Doi: <https://doi.org/10.1096/fasebj.13.1.9>
41. Apte RS, Chen DS, Ferrara N. VEGF in signaling and disease: beyond discovery and development. *Cell*. 2019 Mar 7;176(6):1248-64. Doi: 10.1016/j.cell.2019.01.021
42. Li S, Chen Xi, Wu T, Zhang M, Zhang X, Zongzheng J. Role of heparin on serum VEGF levels and local VEGF contents in reducing the severity of experimental severe acute pancreatitis in rats. *Scandinavian Journal of Gastroenterology*. 2012; 47(2): 237–244. Doi: 10.3109/00365521.2011.647063
43. Birkenhauer E, Neethirajan S. A double-edged sword: the role of VEGF in wound repair and chemoattraction of opportunist pathogens. *International journal of molecular sciences*. 2015 Apr;16(4):7159-72. Doi: 10.3390/ijms16047159
44. Li S, Zhang S, Li R, Chen S, Chang S, Chen X, *et al*. Prophylactic Low-molecular-weight heparin administration protected against severe acute pancreatitis partially by VEGF/Flt-1 signaling in a rat model. *Human & Experimental Toxicology*. 2020;39(10):1345-54. Doi: 10.1177/0960327120919469
45. El-Gohary Y, Gittes G. Structure of islets and vascular relationship to the exocrine pancreas. *Pancreapedia: The Exocrine Pancreas Knowledge Base*. 2018 Jan 16. Doi: 10.3998/panc.2017.10
46. Nandy D, Mukhopadhyay D. Growth factor mediated signaling in pancreatic pathogenesis. *Cancers*. 2011;3(1):841-71. Doi: 10.3390/cancers3010841
47. Khayyat L, Essawy A, Sorour J, Soffar A. Tartrazine induces structural and functional aberrations and genotoxic effects *in vivo*. *PeerJ*. 2017 Feb 23;5: e3041. Doi:10.7717/peerj.3041.
48. Soliman NB. Effect of chronic immobilization stress on the pancreatic structure and the possible protective role of testosterone administration in male albino rats. *Egyptian Journal of Histology*. 2012 Sep 1;35(3):448-57. Doi:10.1097/01.EHX.0000418064.05379.e2
49. Ali AF, Mansour MA, Ali SA, Noya DA. Pancreatic histological changes in adult female albino rats treated with orlistat and the possible protective role of B-carotene. *Egyptian Journal of Histology*. 2021 Sep 1;44(3):643-58. Doi: 10.21608/EJH.2020.40848.1347
50. Schmidt K, Dartsch H, Linder D, Kern HF, Kleene R. A submembranous matrix of proteoglycans on zymogen granule membranes is involved in granule formation in rat pancreatic acinar cells. *Journal of Cell Science*. 2000 Jun 15;113(12):2233-42. Doi: 10.1242/jcs.113.12.2233
51. Ostapenko OV, Kriventsov MA, Shramko YI, Yermola YA, Mostiuk EM. Electron microscopic study of changes in pancreatic exocrine secretory cells in both early and late stages of hypothyroidism. *Russian Open Medical Journal*. 2019;8(3): e0301. Doi: 10.15275/rusomj.2019.0301
52. Sah RP, Dawra RK, Saluja AK. New insights into the pathogenesis of pancreatitis. *Current opinion in gastroenterology*. 2013 Sep;29(5):523-530. Doi: 10.1097/MOG.0b013e328363e399
53. Abonar M, Aboraya A, Elbakary N, Elwan W. Effect of energy drink on the pancreas of adult male albino rat and the possible protective role of avocado oil: Histological and immunohistochemical study. *Egyptian Journal of Histology*. 2022 Jul 1;45(2):386-403. Doi: 10.21608/EJH.2021.59941.1425
54. Rovira M, Scott SG, Liss AS, Jensen J, Thayer SP, Leach SD. Isolation and characterization of centroacinar/terminal ductal progenitor cells in adult mouse pancreas. *Proceedings of the National Academy of Sciences*. 2010 Jan 5;107(1):75-80. Doi: <https://doi.org/10.1073/pnas.0912589107>.

55. Delaspre F, Beer RL, Rovira M, Huang W, Wang G, Gee S, *et al.* Centroacinar cells are progenitors that contribute to endocrine pancreas regeneration. *Diabetes*. 2015 Oct 1;64(10):3499-509. Doi: 10.2337/db15-0153
56. Madankumar A, Jayakumar S, Gokuladhas K, Rajan B, Raghunandhakumar S, Asokkumar S, *et al.* Geraniol modulates tongue and hepatic phase I and phase II conjugation activities and may contribute directly to the chemopreventive activity against experimental oral carcinogenesis. *European Journal of Pharmacology*. 2013; 705: 148–155. Doi: 10.1016/j.ejphar.2013.02.048
57. Kattaia AA, Baset SA. Effect of bisphenol A on the lung of adult male albino rats and the possible protective role of geraniol: a histological and immunohistochemical study. *Egyptian Journal of Histology*. 2014 Mar 1;37(1):24-35. DOI:10.1097/01.EHX.0000444073.66582.1a
58. Stawiarska-Pięta B, Paszczela A, Grucka-Mamczar E, Szaflarska-Stojko E, Birkner E. The effect of antioxidative vitamins A and E and coenzyme Q on the morphological picture of the lungs and pancreata of rats intoxicated with sodium fluoride. *Food and chemical toxicology*. 2009 Oct 1;47(10):2544-50. Doi: 10.1016/j.fct.2009.07.015
59. Marcuzzi A, Crovella S, Pontillo A. Geraniol rescues inflammation in cellular and animal models of mevalonate kinase deficiency. *In vivo*. 2011 Jan 1;25(1):87-92. <http://iv.iiarjournals.org/content/25/1/87>.
60. Eskandari N, Bahramikia S, Mohammadi A, Taati M, Jafarabad SS. Geraniol ameliorated serum lipid profile and improved antioxidant defense system in pancreas, liver, and heart tissues of alloxan induced diabetic rats. *Biologia*. 2022;77(1):241-8. Doi: <https://doi.org/10.1007/s11756-021-00925-4>
61. Elguindy NM, Yacout GA, Elgamal DA. Hepatoprotective impact of geraniol against CCl₄-induced liver fibrosis in rats. *Pakistan Journal of Biological Sciences: PJBS*. 2020 Jan 1;23(12):1650-8. Doi: 10.3923/pjbs.2020.1650.1658
62. Jayachandran M, Chandrasekaran B, Namasivayam N. Geraniol attenuates fibrosis and exerts anti-inflammatory effects on diet induced atherogenesis by NF- κ B signaling pathway. *European journal of pharmacology*. 2015 Sep 5; 762: 102-11. Doi: 10.1016/j.ejphar.2015.05.039
63. Wittig C, Scheuer C, Parakenings J, Menger MD, Laschke MW. Geraniol suppresses angiogenesis by downregulating vascular endothelial growth factor (VEGF)/VEGFR-2 signaling. *PLoS One*. 2015 Jul 8;10(7): e0131946. Doi: 10.1371/journal.pone.0131946

المخلص العربي

تقييم نسيجي وهستوكيميائي مناعي لتأثير الجيرانيل على التغيرات النسيجية المرضية التي يسببها التارترازين في البنكرياس الإفرازي لذكر الجرذ الأبيض البالغ

مرام محمد الكيلاني، دينا فؤاد الشاعر

قسم الهستولوجيا وبيولوجيا الخلية، كلية الطب، جامعة طنطا

المقدمة: التارترازين هي صبغة تلوين طعام اصطناعية من الأزوبنزئين ، وتستخدم على نطاق واسع في الأدوية ومستحضرات التجميل والصناعات الغذائية. وعلى الرغم من مخاطرها الصحية العديدة وتأثيراتها السامة ، فإن تأثير التعرض للتارترازين على الجزء الإفرازي من البنكرياس لا يزال بحاجة إلى مزيد من الدراسة والتوضيح. أما الجيرانيل فهو مركب طبيعي نشط بيولوجيًا ، ومشتق من النباتات. كما أنه مكون شائع في الزيوت الأساسية للعديد من النباتات وله خصائص مضادة للأكسدة و للميكروبات و للبكتيريا وللتهابات ، وكذلك له العديد من الفوائد الصحية. **الهدف من البحث:** تقييم تأثير الجيرانيل ضد التغيرات النسيجية المرضية التي يسببها التارترازين في البنكرياس الإفرازي لذكور الجرذان البيضاء البالغة.

المواد وطرق البحث: لقد تم تقسيم خمسة وأربعين من ذكور الجرذان البيضاء البالغة إلى ٤ مجموعات: المجموعة الضابطة ، مجموعة الجيرانيل (تناولت ٢٠٠ مجم / كجم / يوميًا من الجيرانيل عن طريق الفم لمدة ٣٠ يومًا) ، مجموعة التارترازين (تناولت ٣٠٠ مجم / كجم / يوميًا من التارترازين عن طريق الفم لمدة ٣٠ يومًا) ومجموعة التارترازين والجيرانيل (تناولت التارترازين والجيرانيل بشكل متزامن بنفس الجرعة والمدة مثل المجموعات السابقة). تم تشريح أنسجة البنكرياس وتجهيزها للدراسة النسيجية والهستوكيميائية المناعية.

النتائج: أظهرت مجموعة التارترازين خلايا حويصلات ذات أنوية متقلصة مع ظهور هالة حول الأنوية وفجوات سيتوبلازمية و فقدان للقاعدية السيتوبلازمية مع نقص في الحبيبات الإفرازية. كما لوحظ قنوات متسعة بها إفراز متراكم وأوعية دموية محتقنة وأيضًا تسلل خلوي التهابي مع ازدياد كبير في ترسب الكولاجين. وباستخدام الميكروسكوب الإلكتروني شوهدت أنوية داكنة غير منتظمة مع اتساع في الغشاء المحيط بالنواة و تجاوزيف بالسيتوبلازم وكذلك اتساع في الشبكة الاندوبلازمية الخشنة مع ظهور تغييرات في الحبيبات الإفرازية ،بالإضافة الى اتساع الفراغ بين خلايا الحويصلات. ولقد تسبب التارترازين أيضًا في زيادة في مستوى التفاعل المناعي للـ VEGF. علي الجانب الآخر، أظهر التناول المتزامن للجيرانيل تحسنًا في هذه التغييرات النسيجية.

الخلاصة: أظهرت هذه النتائج أن الجيرانيل له تأثير تحسيني ضد الآثار الضارة للتارترازين على البنكرياس الإفرازي لذكور الجرذان البيضاء البالغة.